
Journal of Computer-Aided Materials Design, **8:** 117–125, 2001.
KLUWER/ESCOM
© 2002 *Kluwer Academic Publishers. Printed in the Netherlands.*

Kinks in the $a/2\langle 111\rangle$ screw dislocation in Ta

GUOFENG WANG, ALEJANDRO STRACHAN, TAHIR ÇAĞIN and
WILLIAM A. GODDARD III*
Materials and Process Simulation Center, Beckman Institute (139-74), California Institute of Technology, Pasadena, CA 91125, U.S.A

Received 15 February 2001; Accepted 1 September 2001

Abstract. We study the structure and formation energy of kinks in the $1/2a\langle 111\rangle$ screw dislocations in metallic Tantalum (Ta) using molecular dynamics with a first principles based many-body interatomic potential. In our study, four $a/3\langle 112\rangle$ kinks are constructed in a quadrupole arrangement in the simulation cell. To the simulation cell, we impose periodic boundary conditions in the directions perpendicular to the [111] direction and fix boundary condition in the [111] direction. We find that two, energetically equivalent, core configurations for the $1/2a\langle 111\rangle$ dislocation lead to 8 distinguishable single kinks and 16 kinds of kink pairs. The different mismatches of the core configurations along [111] direction attributed to the differences in the formation energy for various types of kinks. Formation energies for all possible kinds of isolated single kinks and kink pairs have been determined. It was found that 0.730 eV was the lowest energy cost to form a kink pair in the $a/2\langle 111\rangle$ screw dislocation in Ta.

Keywords: Dislocations, Embedded-Atom-Model Potential, Kinks, Molecular Dynamics, Plasticity

1. Introduction

The behavior of the $a/2\langle 111\rangle$ screw dislocation, whose Burgers vector is $a/2\langle 111\rangle$, in bcc metals has been studied extensively, since its mobility is controlling the plasticity of bcc metals at low temperatures [1–5]. We have previously investigated the core structure, core energy, Peierls energy barrier, and Peierls stress for the $a/2\langle 111\rangle$-screw dislocation in Ta using molecular dynamics (MD) [6]. We found that the Peierls stress is in the order of $10^{-2}\ \mu$ (μ is the bulk shear modulus) at zero temperature. The high Peierls stress accounts for the low mobility of the straight screw dislocations at low temperatures.

At finite temperatures, the flow stress of bcc crystals decreases sharply with the increase in temperature. This is considered as a cause of the ductile-to-brittle transition in these metals [7]. Through the kink pair nucleation and motion process, the dislocations overcome the intrinsically high Peierls potential barriers. The kink pair mechanism for dislocation motion consists of the repeating processes of the kink pair formation and the subsequent migration of two component kinks away from each other. Thus, the kink formation energy rather than the Peierls energy governs the mobility of the screw dislocation in bcc metals at finite temperatures. The accurate determination of the kink formation enthalpies or energies is an important problem both in the experimental and theoretical communities.

For Tantalum, some experimental data on the kink pair formation enthalpy in the $1/2a\langle 111\rangle$-screw dislocation has already been reported. The kink pair formation enthalpy was determined to be 0.92 eV by Funk [8] (using γ relaxation technique), 1.24 eV by Rodrian and Schultz [9]

*To whom correspondence should be addressed: E-mail: wag@wag.caltech.edu

(γ relaxation technique), 0.98 eV by Werner [10] (flow stress dependence on temperature and strain rate) and 0.97 eV by Mizubayashi et al. [11] (anelastic creep measurement). In his two seminal theoretical papers [12, 13], Duesbury studied the structure and Peierls stress of isolated kinks and the formation energy of kink pairs in bcc metal potassium and iron employing atomistic simulations. Duesbury pointed out that the existence of two energetically degenerate core configurations of the $a/2\langle 111\rangle$-screw dislocation leads to six different $a/3\langle 112\rangle$ single kinks.

In this paper, we calculate the formation energy of single kinks and flips (also called anti-phase defect) for the $a/2\langle 111\rangle$-screw dislocation using a first principles based Embedded-Atom-Model potential [14] (named qEAM) for Ta. The complete spectrum of the kink-pair formation energy, which is the summation of the corresponding single kinks and flips, is reported.

The paper is organized in the following way. In Section 2, the simulation model is described in detail. The results and findings are presented in Section 3. The equilibrium dislocation core structures, multiplicity of dislocation defects and formation energies of flips, kinks and kink pairs are discussed in Subsections 3.1, 3.2 and 3.3, respectively. Conclusions are drawn in Section 4.

2. Model of simulation

In order to simulate kinks and anti-phase defects in $1/2a\langle 111\rangle$ screw dislocations, we use orthorhombic simulation cells oriented along three orthogonal crystal directions that are **X**: [11-2], **Y**: [1-10] and **Z**: [111]. Our model crystal consists of three distinct regions in the [111] direction, which is parallel to the dislocation line. The upper and lower regions contain four $a/2\langle 111\rangle$-screw dislocations arranged as a quadrupole; in these regions, different equilibrated dislocations are positioned and oriented providing the appropriate interfacial boundary conditions to generate various types of flips and kinks. The central region contains the defect (kink or flip) on the dislocation. To avoid large initial misfit on the interface between the different regions in our simulation cell, the central region is constructed on the basis of elastic theory and a smooth change of the core configurations along the dislocation is established.

We find that the equilibrium dislocation cores spread out in three $\langle 112\rangle$ directions on $\{110\}$ planes. Since there are six equivalent $\langle 112\rangle$ directions normal to the dislocation line, two kinds of energy degenerate dislocation cores exist. The flip is defined as a defect where a dislocation core configuration changes to the other one along the screw dislocation line [15]; so in our simulation cells the screw dislocations have the same X and Y positions but different relaxed core configurations on either side of the defect. The dislocation with a kink is a dislocation in which one segment lies in an energy minimum position and another segment lies in a neighboring minimum position [16]. The shortest (and lowest energy) kink involves the displacement of the position of the dislocation line in the (111) plane from one equilibrium position to a nearest neighboring equilibrium position; the displacement involved is $1/3a\langle 112\rangle$. Furthermore the screw dislocation might have the same or different core configurations in the upper and lower regions.

In MD simulations, we imposed periodic boundary conditions to the simulation cell in the directions perpendicular to the dislocation line. In all the simulations presented in this paper, we use four dislocations in a quadruple arrangement; we thus have a pair of dislocations with Burgers vector $b = a/2$[111] and two dislocations with Burgers vector $b = a/2$[-1-1-1]

in the same simulation cell. This arrangement minimizes the misfit of atoms at the periodic boundaries and leads to zero total force on dislocations. We use a fix boundary condition in the [111] direction of the simulation cell; we define two $5b$ thick regions where the atom positions are fixed to the relaxed dislocation configuration during the simulation in both ends of the simulation cell. The atoms between two fixed boundaries are allowed to move to minimize total potential energy. The relaxed region needs to be thick enough to minimize the effect of the fixed boundaries on the flip and kink formation energy. We find that the formation energy of the kink typically changes only 0.2% when the cell length along [111] direction is increased from $90b$ to $150b$. In this study, we employed the simulation cell whose geometry was $5a$[11-2], $9a$[1-10] and $150a/2$[111]. Our simulation cell, with a volume $40.7 \times 42.3 \times 431.8$ Å^3, contains 40 500 atoms (37 800 movable atoms) in total.

3. Results and discussion

3.1. Equilibrated dislocation core structure

In our study, the initial screw dislocation quadruple is constructed using the displacements obtained from elasticity theory. Then, the total strain energy of the system was minimized with periodic boundary conditions to obtain the equilibrium core configurations. Using the qEAM force field, we find that the equilibrium dislocation core has three fold symmetry and spreads out in three $\langle 112\rangle$ directions on $\{110\}$ planes in a differential displacement (DD) map. There are 6 equivalent $\langle 112\rangle$ directions on the (111) plane, which lead to two kinds of core configurations both for the dislocation with Burgers vector $a/2$[111] and for the dislocation with Burgers vector $a/2$[-1-1-1]. Figure 1 shows the differential displacement (DD) maps of the different core configurations. Figures 1a and 1b show two cores for a dislocation with $b = 1/2a$[111] and Figs. 1c and 1d show the cores with $b = 1/2a$[-1-1-1]. In DD maps, the atoms are represented by the circles and projected on a (111) plane of the bcc lattice; the arrows indicate the relative displacements, due to the dislocations, in the [111] direction between the neighboring atoms with respect to their positions in the perfect bcc crystal. The direction of the arrow represents the sign of the relative displacement and the magnitude of the arrow is proportional to the relative displacement between the corresponding atoms. When an arrow spans the distance between the two neighboring atoms, the relative displacement between these two atoms is $1/3b$. As we already mentioned, these two types of the dislocation cores are energetically degenerate in the sense both of the core energy and elastic interaction energy. In Fig. 2, we show the atomic displacements in the [111] direction of the relaxed dislocations referenced to the displacements obtained using elasticity theory. Figs. 2a-d correspond to the same cores as those in Fig. 1. The displacement differences for the atoms except the 6 columns of the atoms closest to the dislocation line are less than ± 0.05 Å. This result demonstrates that elastic theory describes the elastic field of the $1/2a\langle 111\rangle$-screw dislocation pretty well and fails at the core region of the dislocation as expected. An important feature seen in Fig. 2 is that the three central atoms of the dislocation translate simultaneously 0.267 Å ($\sim 0.09b$) either in [111] direction or [-1-1-1] direction after the relaxation. This phenomenon is called polarization of dislocation core [17]. The dislocation is named P (positive) type dislocation, if three central atoms shifted along [111] while the dislocation is called N (negative) type dislocation if those three central atoms shifted along [-1-1-1]. Notice that the dislocations have the same polarization regardless of the orientation of Burgers vector b if their cores spread out along the same $\langle 112\rangle$ directions in a DD map. This observation is essential for us

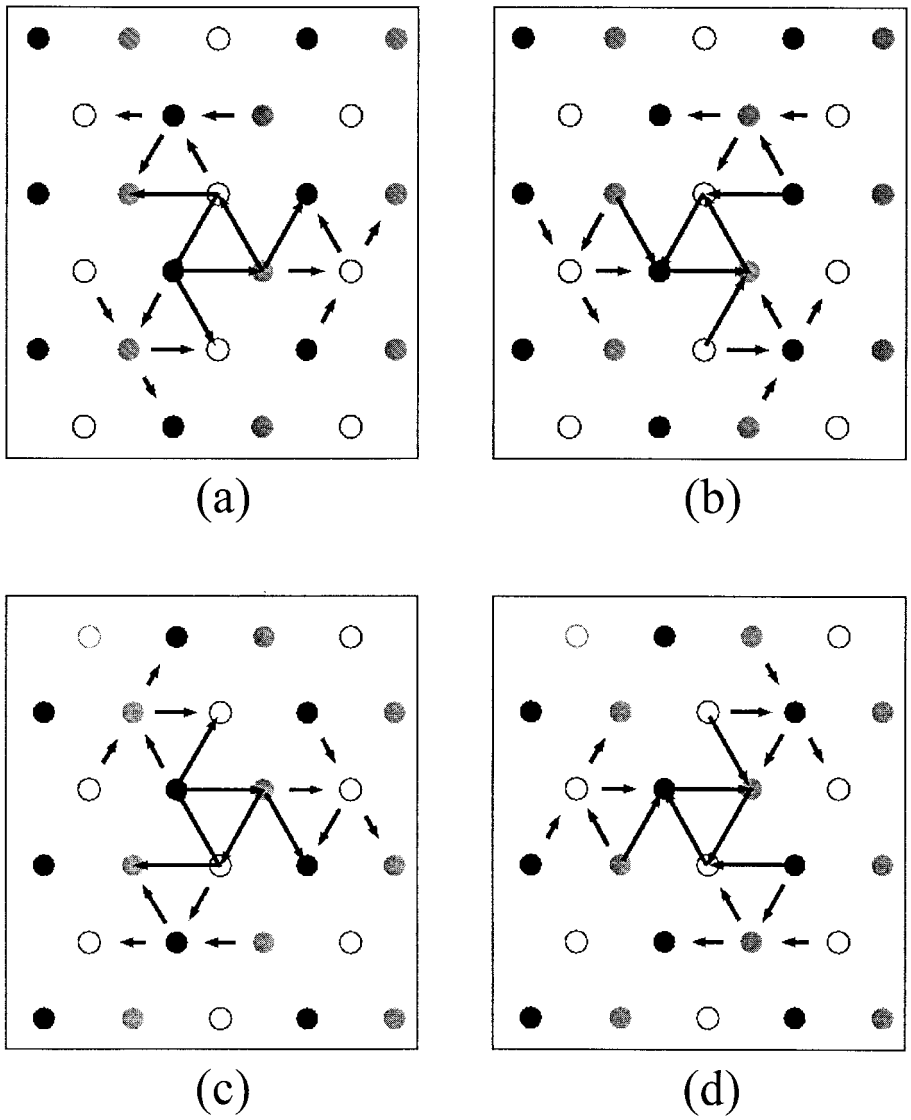

Figure 1. Differential displacement (DD) maps of the equilibrated dislocation core structures. Figure (a) and (b) show two types of core configurations of the dislocation with $b = a/2[111]$, while Figure (c) and (d) show core configurations of the dislocation with $b = a/2[\text{-}1\text{-}1\text{-}1]$.

to guarantee that four dislocations in our simulation cell have the same type of flip or kink defect.

3.2. Multiplicity of dislocation defects

The existence of N-type and P-type dislocations (shown schematically in Fig. 3a) leads to multiple possible configurations of the flips and kinks. Figure 3b shows a diagram of two types of flips as a result of dislocation core polarization. The three columns of atoms closest to the dislocation line are under compression in a P-N flip region and in a tensile state in an N-P flip region. Such that the P-N flip and the N-P flip are two distinct configurations of the $1/2a\langle 111\rangle$ screw dislocation flips. As mentioned, we focused on the kinks where two disloca-

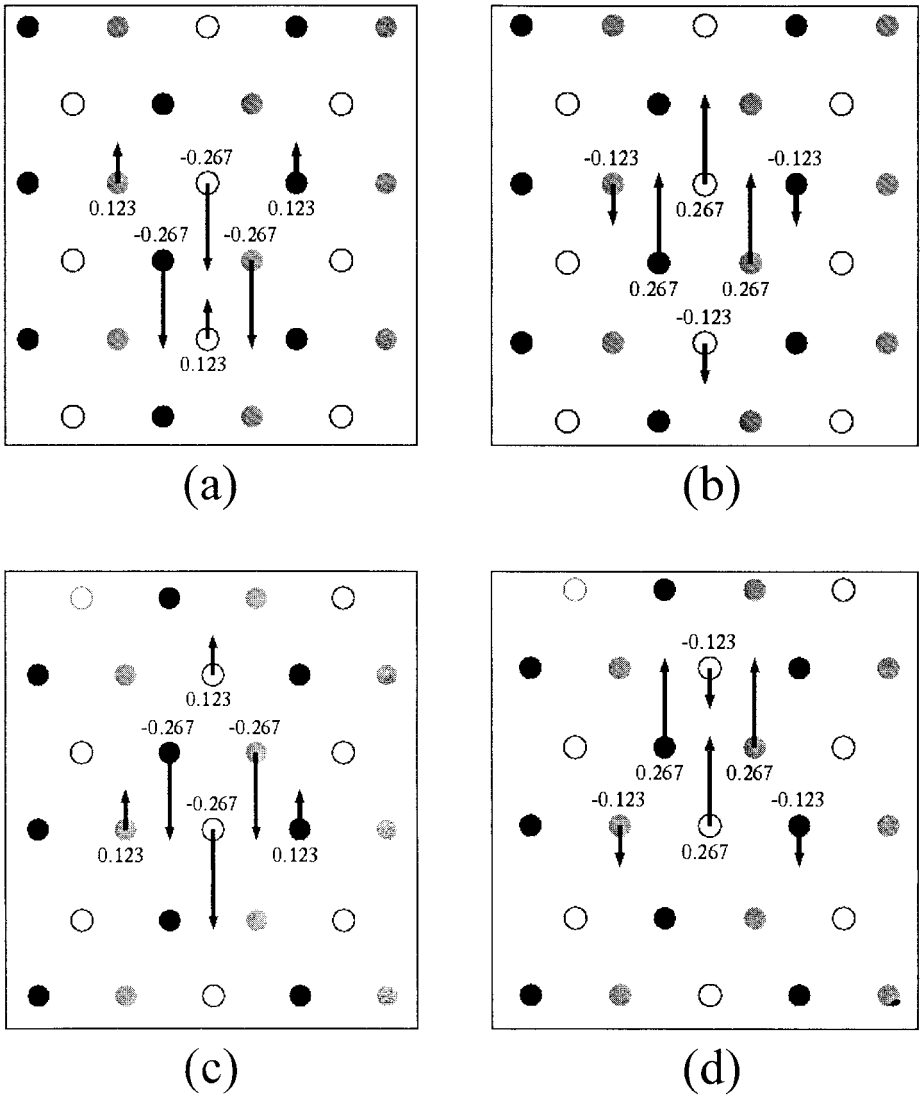

Figure 2. (111) projection of the equilibrium screw dislocation cores. Atoms are represented by circles and projected on a (111) plane of bcc lattice. The arrow from each atom indicates the relaxation parallel to the dislocation line relative to the displacement field predicted by isotropic elastic theory. The relaxation magnitudes of the central six columns of atoms are printed next to the corresponding atom and in the unit of Å. The arrangement of the figure is the same as in Figure 1.

tion segments are in the nearest neighbor equilibrium positions (separated by $a/3\langle 112\rangle$). We define the kink vector as the vector that goes from the equilibrium dislocation position below the kink to the equilibrium dislocation position above the kink. There are six possible $\langle 112\rangle$ directions but only two need to be considered by symmetry, this leads to two kink directions which we will call left (with kink vector $-a/3$[11-2]) and right (with kink vector $a/3$[11-2]). For each kink vector, there are four combinations of core configurations leading to 8 possible kinks: NRP, NRN, PRP, PRN, NLP, NLN, PLP, and PLN. All possible distinct $a/3\langle 112\rangle$ single kinks are shown in the Fig. 3c. Among these kinks, the NRN kink and the PRP kink are energy degenerate and related by symmetry operations, so are the NLN kink and the PLP kink.

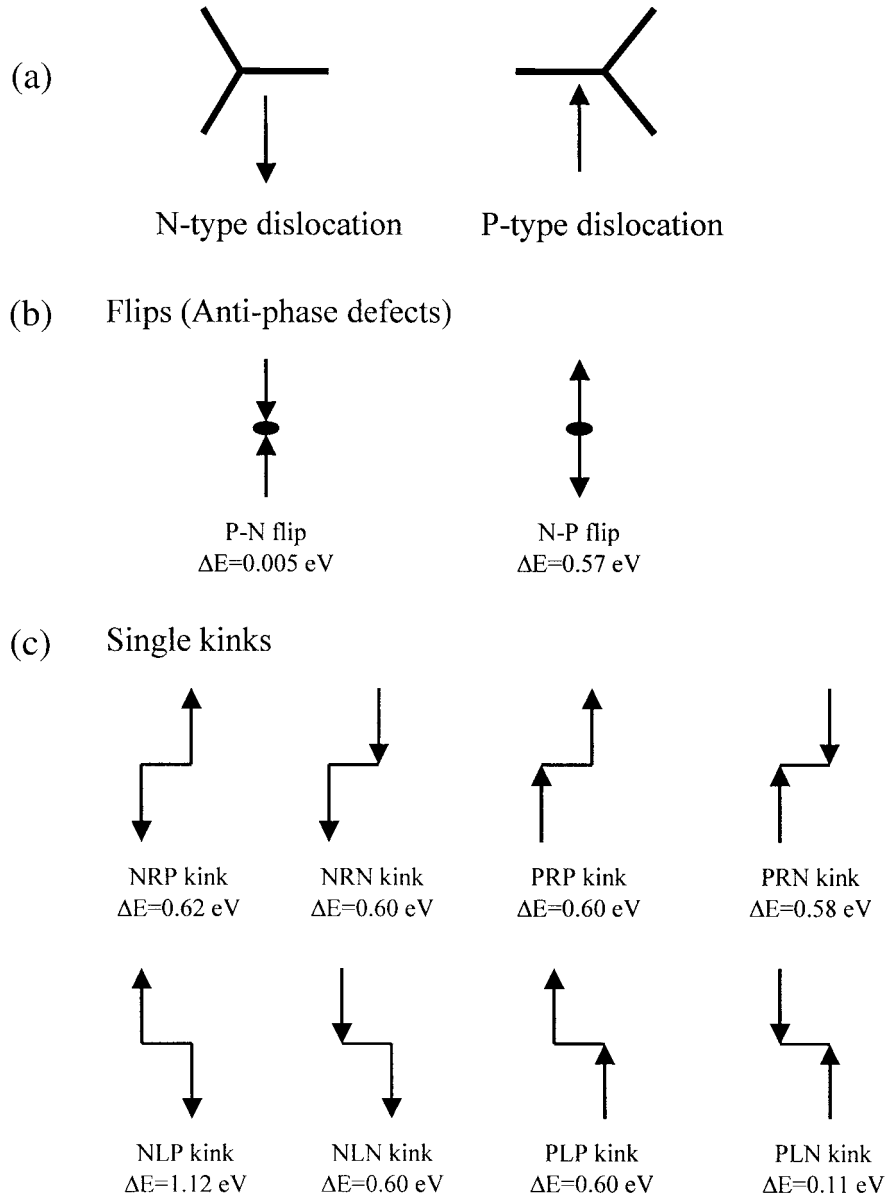

Figure 3. (a) Schematic drawings of N-type dislocation core and P-type dislocation core. Arrows indicate whether three central columns of atoms move inward or outward defect (flip or kink) region. (b) Sketches and formation energies of the flips. (c) Sketches and formation energies of the isolated single kinks.

3.3. Formation energy of flips, kinks and kink pairs

The dislocation core configurations, their polarization and the multiplicity of flips and kinks have been discussed in the previous sections. With this knowledge, it is practical to obtain an equilibrated dislocation quadruple in the way described in Section 2 such that all four dislocations have the same type of flips or kinks. The total strain energy of the equilibrated dislocation quadruple with defects can be expressed as the summation of the formation energy

Table 1. Schematic drawings and formation energies of kink-pairs. Formation energies are printed in the figure and in the unit of eV. n and p stands for N-type or P-type dislocation core, respectively. nxp and pxn represent N-P flip or P-N flip.

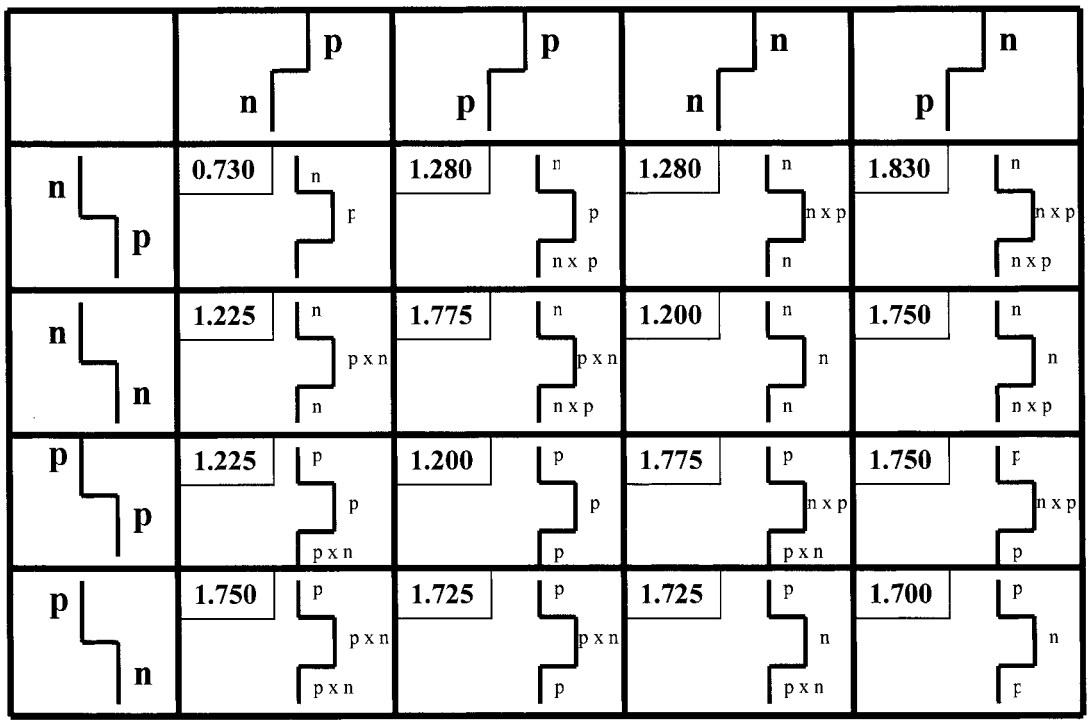

of the defects (flip or kink), the elastic interaction energy between the defects and the energy of the quadrupolar perfect dislocations.

The elastic interaction energy between flips is zero because the dislocation line remains unchanged and so does its elastic field. Thus, the formation energy of flips is simply the total energy of the quadrupolar dislocations with flips minus that of the perfect dislocations divided by four. Figure 3b shows the results obtained with our qEAM force field.

The interaction energy between kinks is not zero because the kink is a one-dimensional line segment. Nevertheless, as a first order approximation, we neglect their interaction and calculate the kink formation energy similarly as it was explained for the flips. The resulting formation energies are shown in Fig. 3c. The systematic error introduced by neglecting the elastic interactions for a periodic kink quadruple can be estimated using the isotropic elastic theory and assuming that the kinks are the pure $\langle 112\rangle$ edge segments perpendicular to the dislocation lines. [16] For our simulation cell, we estimate the kink interaction energy to be -0.03 eV, i.e., the kink formation energies shown in Fig. 3c should be increased by 0.003 eV. It is worth mentioning here that the equilibrated kink is not simply an edge segment perpendicular to the dislocation line. Actually, the kink has a very large screw component; we find that the kink length in the [111] direction is $\sim 10b$ ($\sim$28.8 Å), an order of magnitude larger than its extent in the $\langle 112\rangle$ direction ($\sim$2.71 Å). Thus, the expected systematical error in computing the kink formation energy in our study is much smaller than our estimation of

0.03 eV. In Fig. 3, the flips and kinks are drawn schematically showing the core configuration misfit.

In addition to the single kink at which the dislocation line lies across a Peierls energy hill, there are kink pairs constituted by a pair of left kink and right kink. These kink pairs can be formed in materials by thermal fluctuation and their nucleation and motion are thought to be important in low temperature deformation processes [16]. If the separation between the component left and right kink is large enough, the formation energy of a kink pair is just the sum of the formation energy of these two component kinks. Since there are 4 kinds of left kinks and 4 kinds of right kinks, there are 16 ways to combine them to form kink pairs. In some cases, one or two flips are required to fulfill the requirement of the core configuration of the dislocation. Table 1 lists the configurations and formation energies for all kink pairs. We find that the NRP-PLN kink pair has the lowest formation energy which is 0.73 eV, which is 0.47 eV less than the second lowest formation energy for a NRN-NLN kink pair (or PRP-PLP kink pair).

4. Concluding remarks

In summary, we found that there were two types of the equilibrated core configurations for the $a/2\langle 111\rangle$-screw dislocation. These two energy degenerate core configurations lead to the opposite polarizations, namely three columns of the atoms closest to these two types of dislocation lines translate simultaneously in the opposite [111] directions with respect to the displacements obtained from the elasticity theory. Two types of dislocation core configurations lead to 2 kinds of dislocation flips and 8 kinds of dislocation single kinks. We calculated the formation energies for these dislocation defects by minimizing the energy of a dislocation quadruple containing the defects to an equilibrated state. The kink pairs are the combination of a pair of left and right single kinks plus one or two flips that adjust the dislocation core configurations. We have computed formation energies for all 16 kinds of kink pairs and found that the NRP-PLN kink pair has the lowest nucleation energy, 0.73 eV. We found that the formation energies of the right kinks [NRP, NRN (PRP) and PRN] are very similar, differing only by 0.02 eV from one to the other. On the other hand, the formation energy of the left kinks [PLN, PLP (NLN) and NLP] differ by approximately 0.50 eV. The different behavior of the left and right kinks can be explained by analyzing their core structures. We find that the PLP kink ($\Delta E = 0.6$ eV) is formed by a PLN kink ($\Delta E = 0.11$ eV) plus a NP flip ($\Delta E = 0.57$ eV) in a very short distance. The NLP kink ($\Delta E = 1.12$ eV) is formed by a NP flip ($\Delta E = 0.5$ eV), a PLN kink ($\Delta E = 0.11$ eV) and another NP flip ($\Delta E = 0.5$ eV) along the dislocation line. The presence of the NP flip explains the large energy differences among the left kinks. While the right kinks differ by the low energy PN flip ($\Delta E = 0.005$ eV) and they have very similar formation energies. A detailed structural analysis of the different kinks will be published elsewhere [18].

Acknowledgements

This research was funded by a grant from DOE-ASCI-ASAP. The facilities of the MSC are also supported by grants from NSF (CHE 9985574 and CHE 9977872), ARO (MURI), ARO (DURIP), Chevron Corp., Seiko Epson, Dow Chemical, Avery Dennison, 3M, General Motors, Kellogg's Beckman Institute, and Asahi Chemical.

References

1. Vitek, V., Crystal Lattice Defects, 5 (1974) 1.
2. Xu, W. and Moriarty, J.A., Phys. Rev., B54 (1996) 6941.
3. Xu, W. and Moriarty, J.A., Comput. Mater. Sci., 9 (1998) 348.
4. Moriarty, J.A., Xu, W., Söderlind, P., Belak, J., Yang, L.H. and Zhu, J., Eng. Mater. Technol., 121 (1999) 120.
5. Ismail-Beigi, S. and Arias, T.A., Phys. Rev. Lett., 84 (2000) 1499.
6. Wang, G., Strachan A., Çagin, T. and Goddard, W.A., Mater. Sci. and Eng., A309 (2001) 133.
7. Wen, M. and Ngan, A.H.W., Acta Mater., 48 (2000) 4255.
8. Funk, G., Dissertation, University Stuttgart, 1985.
9. Rodrian, U. and Schultz, H., Z. Metallk., 73 (1982) 21.
10. Werner, M., Phys. Stat. Sol. (a), 104 (1987) 63.
11. Mizubayashi, H., Egashira, H. and Okuda, S., Acta Metall. Mater., 43 (1995) 269.
12. Duesbery, M.S., Acta Metall., 31 (1983) 1747.
13. Duesbery, M.S., Acta Metall., 31 (1983) 1759.
14. Strachan A., Çagin, T., Gulseren, O., Mukherjee, S., Cohen, R.E. and Goddard W.A., Phys. Rev. B, submitted.
15. Hirth, J.P., Acta Mater., 48 (2000) 93.
16. Hirth, J.P. and Lothe, J., Theory of Dislocations, Krieger, Melbourne, FL, 1992.
17. Seeger, A. and Wuthrich, C., Nuovo Cimento, 33 (1976) 38.
18. Wang, G., Strachan A., Çagin, T. and Goddard, W.A., in preparation.